Published in final edited form as:
Eur J Immunol. 2013 January ; 43(1): 65–74. doi:10.1002/eji.201242379.

GILT expression in B cells diminishes cathepsin S steady-state protein expression and activity

Hannah Phipps-Yonas[1,2], **Vikki Semik**[1], and **Karen Taraszka Hastings**[1,2,3]

[1]Department of Basic Medical Sciences, College of Medicine-Phoenix, University of Arizona, Phoenix, Arizona, USA

[2]Arizona Cancer Center, College of Medicine, University of Arizona, Tucson, Arizona, USA

[3]Department of Immunobiology, College of Medicine, University of Arizona, Tucson, Arizona, USA

Abstract

MHC class II-restricted Ag processing requires protein degradation in the endocytic pathway for the activation of $CD4^+$ T cells. Gamma-interferon-inducible lysosomal thiol reductase (GILT) facilitates Ag processing by reducing protein disulfide bonds in this compartment. Lysosomal cysteine protease cathepsin S (CatS) contains disulfide bonds and mediates essential steps in MHC class II-restricted processing, including proteolysis of large polypeptides and cleavage of the invariant chain. We sought to determine whether GILT's reductase activity regulates CatS expression and function. Confocal microscopy confirmed that GILT and CatS colocalized within lysosomes of B cells. GILT expression posttranscriptionally decreased the steady-state protein expression of CatS in primary B cells and B-cell lines. GILT did not substantially alter the expression of other lysosomal proteins, including H2-M, H2-O, or CatL. GILT's reductase active site was necessary for diminished CatS protein levels, and GILT expression decreased the half-life of CatS, suggesting that GILT-mediated reduction of protein disulfide bonds enhances CatS degradation. GILT expression decreased the proteolysis of a CatS selective substrate. This study illustrates a physiologic mechanism that regulates CatS and has implications for fine tuning MHC class II-restricted Ag processing and for the development of CatS inhibitors, which are under investigation for the treatment of autoimmune disease.

Keywords

Antigen presentation/processing; Antigen presenting cells; B cells; Cathepsin S; Gamma-interferon-inducible lysosomal thiol reductase (GILT)

Introduction

Activation of $CD4^+$ T cells requires the presentation of peptides in the context of MHC class II molecules on professional APCs (reviewed in [1]). MHC class II αβ heterodimers are assembled in the endoplasmic reticulum in association with invariant chain (Ii) [2]. The cytoplasmic tail of Ii targets the MHC class II-Ii complex into the endocytic pathway, where

Correspondence: Dr. Karen Taraszka Hastings, 425 N. 5th St., Phoenix, AZ 85004, USA, Fax: +1-602-827-2127, khasting@email.arizona.edu.

Conflict of interest: The authors declare no financial or commercial conflict of interest.

Additional supporting information may be found in the online version of this article at the publisher's web-site

Ii is sequentially cleaved leaving CLIP (class II-associated invariant chain peptides) associated with the MHC class II peptide binding groove [3–9]. Lysosomal proteases known as cathepsins (CatS) are responsible for the cleavage of Ii and the proteolysis of endocytosed and endogenous proteins in this compartment [10–15]. Reduction of protein disulfide bonds in the lysosomal compartment by gamma-interferon-inducible lysosomal thiol reductase (GILT) facilitates the generation of MHC class II-restricted epitopes from disulfide bond-containing protein Ags, such as tyrosinase-related protein-1, which is an autoAg in vitiligo and a tumor Ag in melanoma [16–18]. H2-M (HLA-DM in humans) mediates the removal of CLIP and stabilizes MHC class II until a high-affinity peptide is bound [19,20]. H2-O (HLA-DO in humans) associates with H2-M and negatively regulates its function [21, 22]. Peptide-MHC class II complexes are transported to the cell surface for stimulation of $CD4^+$ T cells.

GILT is constitutively expressed in most APCs and is upregulated by IFN-γ in other cell types such as melanoma cells [17, 23–25]. GILT is synthesized as a 35 kDa precursor and targeted to lysosomes by mannose-6-phosphate tagging [17, 23]. In early endosomes, cleavage of *N*- and *C*-terminal propeptides generates the 28 kDa mature form that localizes to late endosomes and lysosomes [17,23,26,27]. GILT catalyzes disulfide bond reduction with optimal activity at an acidic pH and is the only known reductase localized to the endocytic pathway [23]. GILT's reductase active site is composed of a thioredoxin-like CXXC motif, corresponding to Cys-46 and Cys-49 in the mature form of human GILT [23]. Similar to thioredoxin, the thiol group of the *N*-terminal cysteine initiates a nucleophilic attack on the substrate disulfide bond, a GILT-substrate mixed disulfide intermediate is formed, and intramolecular attack from the thiol of the *C*-terminal cysteine results in release of the reduced substrate [26]. Reduction of protein disulfide bonds in the endocytic pathway is hypothesized to facilitate MHC class II-restricted processing through exposing buried epitopes for MHC class II binding. GILT-mediated protein disulfide bond reduction in phagosomes also facilitates transfer of disulfide-containing Ags into the cytosol enhancing cross-presentation of exogenous proteins on MHC class I [28]. Furthermore, GILT accelerates autoimmunity and alters tolerance of $CD4^+$ T cells recognizing GILT-dependent epitopes [18, 29].

Our previous work demonstrates that reductase active site mutants of GILT in murine B cells have diminished processing of precursor GILT to its mature form [16], suggesting the possibility that GILT's reductase active site may play an indirect role in GILT maturation by altering the expression of, or maintaining the activity of, lysosomal proteases. Multiple Cats are capable of mediating the cleavage of the *N*- and *C*-terminal propeptides of precursor GILT in vitro [26]. In vivo data support the redundancy of CatS in mediating GILT maturation, as cleavage of precursor GILT is not significantly delayed in $CatS^{-/-}$ B cells [25]. In addition, GILT has been reported to influence Cat levels in melanoma cell lines [30]. Therefore, we sought to test the hypothesis that GILT's reductase active site regulates the expression or activity of lysosomal CatS in professional APCs. We focused on cysteine protease CatS given its importance in MHC class II-restricted presentation. $CatS^{-/-}$ peripheral APCs have reduced Ii degradation and altered processing of soluble exogenous Ags [13, 14]. In contrast, CatB and CatD are not necessary for Ii degradation and MHC class II-restricted processing [31,32]. In this study, we identified a previously unknown level of regulation of CatS that involves GILT.

Results

GILT and CatS colocalize in lysosomes of primary B cells

To evaluate a possible interaction between GILT and CatS, we first confirmed the subcellular localization of GILT in primary murine B cells. Prior electron microscopy

studies have shown that GILT localizes to both multivesicular late endosomes and multilaminar lysosomes in B cells [23]. WT splenic B cells stained with anti-GILT serum (Fig. 1A, red) and anti-lysosome-associated membrane protein-1 (LAMP-1) mAb (Fig. 1A, green) revealed a punctate pattern consistent with localization to the late endosomes and lysosomes. The merged images demonstrated the colocalization of GILT and LAMP-1 (Fig. 1A, yellow). We quantified the degree of colocalization using Image J software with the JACoP plugin. The Manders coefficient for the fraction of GILT signal that colocalized with LAMP-1 was 0.93 ± 0.06 (mean ± SD). Next, we determined whether GILT and CatS colocalize in primary B cells. Staining with anti-GILT serum and anti-CatS Ab in WT B cells both showed a punctate pattern (Fig. 1B, green and red, respectively). Merged images demonstrated the colocalization of GILT and CatS (Fig. 1B, yellow). The Manders coefficient for the fraction of GILT signal that overlapped with CatS was 0.99 ± 0.01. Z-stack imaging showed that the colocalization of GILT and CatS was consistent throughout the cell (data not shown). B cells from GILT$^{-/-}$ mice maintained CatS expression and served as a negative control for GILT (Fig. 1B, bottom row). In each case, no staining was observed with the secondary Ab alone (data not shown). These findings are consistent with studies showing the colocalization of GILT with other lysosomal cysteine proteases CatB and CatD in human melanoma cell lines [30]. These data demonstrate the colocalization of GILT and CatS in the lysosomal compartments of primary B cells and allow for a possible interaction between the two proteins that could modulate CatS expression and function.

GILT posttranscriptionally decreases the steady-state protein expression of CatS in primary B cells

To determine whether GILT expression affects the steady-state protein levels of CatS, WT and GILT$^{-/-}$ primary B-cell lysates were analyzed by immunoblotting for CatS. A single 26 kDa band representing mature CatS was observed in both WT and GILT$^{-/-}$ B cells (Fig. 2A), as observed in murine dendritic cells [33]. The steady-state protein expression of CatS was increased in B cells lacking GILT in three independent sets of lysates (Fig. 2A). CatS signal intensities relative to GRP94 were estimated to be approximately three times higher in GILT$^{-/-}$ B cells compared with that of WT B cells (Fig. 2B). In a previous study of human melanoma cell lines, transfection with GILT did not substantially alter CatS steady-state protein levels [30]. This difference may be due to differences in cell type (professional APC versus aberrant MHC class II expression in a cancer cell line), CatS expression, and/or MHC class II alleles. To begin to examine the mechanism of GILT's effect on CatS, we quantified CatS transcripts in mRNA isolated from WT and GILT$^{-/-}$ primary B cells to determine whether GILT expression affects CatS transcription or diminishes CatS expression posttranscription. There was no significant difference in the CatS mRNA levels between WT and GILT$^{-/-}$ B cells (Fig. 2C), indicating that GILT acts posttranscriptionally to decrease the steady-state protein levels of CatS.

To identify whether GILT's effect is limited to CatS or whether GILT affects multiple lysosomal proteins involved in MHC class II loading, we evaluated the effect of GILT expression on MHC class II-like molecules H2-M and H2-O. There was no statistically significant difference in the steady-state level of H2-Mα or H2-Oβ in the presence and absence of GILT (Fig. 2D and E). Next, we evaluated GILT's effect on expression of CatL, a lysosomal cysteine protease that is necessary for Ii degradation in cortical thymic epithelial cells, but not in bone marrow-derived APCs [34]. Lysates from WT and GILT$^{-/-}$ thymuses were immunoblotted with anti-CatL serum. In the thymus, multiple forms of CatL were identified corresponding to the described precursor form (doublet at 36 kDa), the 28 kDa single chain mature form, and the 21 kDa heavy chain of the two-chain mature form (Fig. 2F) [35]. There was no statistically significant difference between the level of each form of CatL found in WT compared with GILT$^{-/-}$ thymuses (Fig. 2F). Consistent with previous

studies that have identified a single mature form of CatL in murine B cells [25], a single band corresponding to mature CatL was observed in WT and GILT$^{-/-}$ B cells (Fig. 2G). In addition to a possible effect of GILT expression, an increase in CatL expression could be due to decreased CatS expression, as CatS$^{-/-}$ B cells have increased CatL protein expression [25]. However, no significant difference in the steady-state protein level of mature CatL was observed between WT and GILT$^{-/-}$ B cells (Fig. 2G). These data indicate that GILT does not substantially alter the steady-state protein expression of H2-M, H2–O, or CatL.

Expression of GILT is sufficient to diminish steady-state levels of CatS

To determine whether differences in the types of B cells, which in turn may express different levels of CatS, may account for the difference in CatS levels in primary B cells, we evaluated the percentage of CD21^{+}CD23^{+} follicular B cells and CD21^{hi}CD23^{lo} marginal zone B cells within the CD19^{+} B-cell gate from WT and GILT$^{-/-}$ splenocytes (Supporting Information Fig. 1). There was no difference in the percentage of follicular B cells; the percentage of follicular B cells was 75.0 ± 1.5 (mean ± SD) and 73.3 ± 1.8 from WT and GILT$^{-/-}$ mice, respectively. There was a small, but statistically significant increase in the percentage of marginal zone B cells in GILT$^{-/-}$ compared with WT splenic B cells (11.1 ± 0.8 versus 7.2 ± 1.0; $n = 6$ mice per group; $p < 0.05$). The significance of this difference is uncertain. While the approximately 4% increase in the percentage of marginal zone B cells may contribute to a difference in CatS levels, it is unlikely to account for the entire threefold increase in CatS levels in B cells from GILT$^{-/-}$ mice. To further investigate this possibility, we examined the effect of expressing GILT in a GILT$^{-/-}$ B-cell line on CatS protein levels.

To definitively demonstrate that the addition of GILT is sufficient to diminish steady-state levels of CatS, we transduced the GILT$^{-/-}$ B-cell line BμMyc.GKO.1 [16] with WT GILT or vector alone. Following transduction with GILT, both precursor and mature forms of GILT were detected (Fig. 3A), as previously observed in these cells and the murine A20 B-cell lymphoma line [16,17]. Immunoblot analysis showed that the GILT$^{-/-}$ B-cell line transduced with WT GILT had a 3.7-fold decrease in steady-state protein level of CatS compared with those transduced with vector alone (Fig. 3B, lanes 1 and 2, and Fig. 3C, columns 1 and 2), validating results found in primary B cells (Fig. 2). These data confirm that GILT expression is sufficient to decrease intracellular CatS steady-state protein expression.

GILT's reductase active site is necessary for diminished CatS protein expression

To determine whether GILT's reductase active site was required for decreased CatS expression, we transduced the GILT$^{-/-}$ B-cell line BμMyc.GKO.1 with WT GILT or cysteine mutants of the reductase active site [16]. We previously demonstrated that these WT and mutant GILT constructs colocalize with MHC class II and LAMP-1 in BμMyc.GKO.1 cells [16]. In each experiment, the transduction efficiency was determined to be uniformly greater than 90% (Supporting Information Fig. 2). WT GILT and all three active site cysteine mutants were equivalently expressed at steady state (Fig. 3A, lanes 2–5). Mature GILT was the predominant form at steady state (Fig. 3A, lanes 2–5). The precursor form was detected as a doublet, which may be due to variable *N*-linked glycosylation as seen with GILT overexpression in COS-7 cells [26] (Fig. 3A, lanes 2–5). There was a small increase in the precursor relative to the mature form in mutants C46S and C46SC49S (Fig. 3A, lanes 3 and 5), consistent with mutation of GILT's reductase active site resulting in diminished GILT maturation [16]. In contrast to transduction with WT GILT that resulted in decreased CatS protein levels, transduction with mutant GILT (C46S, C49S, or C46SC49S) did not alter CatS steady-state protein expression compared with transduction with vector alone (Fig. 3B, lanes 1 and 3–5, and Fig. 3C). These data confirm that decreased CatS protein expression is dependent on an intact reductase active site of GILT.

GILT decreases the stability of CatS

Since CatS has three disulfide bonds that maintain its tertiary structure [36], we hypothesized that GILT-mediated reduction of CatS may decrease the half-life of CatS resulting in diminished steady-state levels of CatS. To evaluate whether GILT decreased the half-life of CatS, we first attempted ^{35}S labeling and pulse-chase analysis; however, we were not able to detect CatS protein with ^{35}S labeling and immunoprecipitation. Next, we examined CatS protein levels in GILT$^{-/-}$ BμMyc.GKO.1 B cells transduced with vector alone or WT GILT following inhibition of translation with cycloheximide. Figure 4 A and B show immunoblots for CatS from lysates of GILT$^{-/-}$ B cells transduced with vector alone or WT GILT, respectively. In each case, lysates from GILT-expressing and GILT-deficient B cells are shown at the zero time point, demonstrating decreased steady-state CatS expression in the presence of GILT (Fig. 4A and B, lanes 1 and 2). In GILT-deficient B cells, we observed no change in CatS steady-state levels over 9 h of cycloheximide treatment (Fig. 4A and C). In contrast, in the presence of GILT, CatS steady-state levels were diminished by approximately 50 and 70% after 6 and 9 h of cycloheximide treatment, respectively (Fig. 4B and C). These data show that the half-life of CatS is decreased in the presence of GILT.

GILT decreases the proteolysis of a CatS-selective substrate in primary B cells

Since GILT expression reduced the steady-state levels of CatS protein, we hypothesized that GILT expression would diminish CatS function on a per cell basis. We used a fluorescence-based protease activity assay in which the activity of CatS, CatB, and CatL in cell lysates is measured by quantifying the release of fluorescent free amino-4-trifluoromethyl coumarin (AFC) resulting from the cleavage of a Cat selective substrate. The 47% increase in CatS protease activity in the lysates of GILT$^{-/-}$ primary B cells compared with that of WT B cells was highly significant ($p < 0.0001$) (Fig. 5, left). A caveat in the interpretation of this result is that the small increase in marginal zone B cells found in GILT$^{-/-}$ splenic B cells may contribute in part to this finding (Supporting Information Fig. 1). As another approach to assess the specificity of GILT's effect, we assessed the effect of GILT expression in primary B cells on CatB and CatL activity. Overall, the levels of CatB and CatL activity were fivefold lower than CatS (Fig. 5). High levels of CatB detected by cysteine protease active site labeling in B cells [13,25] did not translate to high levels of substrate cleavage in this assay. Low CatL activity in APCs is consistent with previous reports [25, 34, 37]. Lysates from WT and GILT$^{-/-}$ B cells displayed no significant difference in CatB activity (Fig. 5, middle). Although we did not detect a difference in CatL protein expression (Fig. 2G), a smaller 24% increase in CatL protease activity was observed in the lysates of GILT$^{-/-}$ compared with those from WT B cells ($p < 0.01$) (Fig. 5, right). In each case, protease activity was abolished with inclusion of a Cat inhibitor. Together these data indicate that GILT expression decreases the steady-state protein expression of CatS resulting in less CatS protease activity per cell equivalent.

Discussion

GILT and CatS are both localized in the lysosomal compartment and have important functions in MHC class II-restricted Ag processing. We demonstrate that CatS steady-state protein levels are diminished in WT compared with GILT$^{-/-}$ primary B cells and that GILT expression in a B-cell line is sufficient to diminish CatS steady-state protein levels. After excluding the possibility that GILT expression reduced CatS transcription, we determined that the ability of GILT to diminish CatS steady-state protein levels was dependent on GILT's reductase active site and that the half-life of CatS is shortened in the presence of GILT. Since CatS has three disulfide bonds that contribute to maintaining the tertiary structure of CatS [36], a potential mechanism of GILT's effect is that CatS may be a substrate of GILT and GILT-mediated reduction of CatS may decrease the stability of CatS.

Alternatively, GILT expression may indirectly diminish the stability of CatS. Immunoprecipitation and immunoblot for CatS, as well as CatS activity assays, from supernatants of GILT-deficient and GILT-expressing B cells did not provide evidence for altered CatS secretion (data not shown). These studies demonstrate a previously unreported role for GILT in regulating CatS levels; however, the exact molecular mechanism by which GILT regulates CatS levels remains to be elucidated.

Decreased CatS protein levels correspond with decreased CatS protease activity in GILT-expressing B cells. CatS enhances MHC class II-restricted processing through cleavage of Ii and digestion of large polypeptides [12–15]. We took two approaches to determine whether decreased CatS activity corresponds with a change in Ii processing. First, immunoblots to measure Ii proteolytic intermediates in GILT-deficient and GILT-expressing B cells were performed. Second, we performed flow cytometric analysis to measure cell surface expression of MHC class II I-A^b bound to Ii degradation intermediates p12 and CLIP. However, no differences in Ii proteolysis or expression of Ii fragments on the cell surface were detected (data not shown). Given that Ii is highly susceptible to lysosomal degradation, that multiple proteases can perform this role, and that Ii proteolysis continues in the absence of CatS [13], it is not surprising that we were unable to detect a difference in Ii proteolysis with a threefold decrease in CatS protein levels in GILT-expressing cells. Nonetheless, our data show that in the presence of GILT, CatS stability is diminished and CatS activity on a per cell basis with a more sensitive synthetic substrate is decreased. The impact of GILT regulation of CatS on Ag processing and presentation remains to be determined and will be the subject of future studies.

The alteration of lysosomal proteolysis has implications for MHC class II-restricted processing and presentation. Given that GILT facilitates the presentation of certain epitopes from disulfide bond-containing protein Ags [17, 18, 24, 38] and CatS promotes MHC class II-restricted processing [12–15], it may seem to be an apparent paradox that GILT expression decreases CatS expression and function. However, fine control of lysosomal proteolysis is required for optimal Ag presentation, as lysosomal proteases have both the ability to generate and destroy immunogenic epitopes [39]. We show here that GILT contributes to the control of lysosomal protease activity. In addition, efficient MHC class II-restricted presentation depends on the inflammatory milieu and activation of the APC [33,40]. It is possible that GILT suppresses the MHC class II-restricted presentation of endogenous proteins in resting B cells. This hypothesis is supported by a mass spectrometric analysis of MHC class II bound peptides eluted from resting WT and $GILT^{-/-}$ splenocytes, of which resting B cells compose the predominate MHC class II-positive cell type. No unique peptides were identified from WT splenocytes, and 95% of the peptides were more abundant on $GILT^{-/-}$ splenocytes including 2% that were exclusively identified from $GILT^{-/-}$ splenocytes [41]. In addition to GILT's role in facilitating presentation of certain epitopes from disulfide bond-containing protein Ags, we show that GILT's reductase active site diminishes CatS protein levels by decreasing CatS stability. GILT may fine tune Ag presentation by modulating lysosomal proteolysis.

Modulation of Ag presentation and, in particular, inhibition of CatS activity are under investigation as therapeutic approaches for autoimmune disease. The initial descriptions of Cat function in Ag presentation in vivo suggested selective inhibition of these cysteine proteases as a therapeutic strategy for manipulating $CD4^+$ T-cell responses and treating autoimmune diseases [13, 15, 34]. These reports demonstrate that inhibition or knockout of CatS reduced T cell-dependent Ab responses, pulmonary hypersensitivity, and collagen-induced arthritis in mouse models [13, 15]. A more recent study demonstrates that a CatS inhibitor blocks lymphocytic infiltration of lacrimal and salivary glands and autoAb formation in a mouse model of Sjögren syndrome [42]. Also, CatS inhibition after

sensitization with myelin oligodendrocyte glycoprotein$_{35–55}$ peptide delays the onset and progression of murine experimental autoimmune encephalomyelitis, and treatment of established collagen-induced arthritis with a CatS inhibitor results in an improved clinical score and reduced bone loss in mice [43]. Furthermore, the safety and efficacy of a CatS inhibitor has been tested in a clinical trial of patients with active rheumatoid arthritis (clinicaltrails.gov). Cystatin C is an endogenous inhibitor of CatS [44]; however, cystatin C levels do not control MHC class II-restricted Ag presentation [45]. Our study illustrates a previously unreported physiologic mechanism responsible for regulating CatS steady-state protein levels and activity.

Materials and methods

Animals and cells

C57BL/6 (WT) mice were obtained from Jackson Laboratory (Sacramento, CA, USA). GILT$^{-/-}$ mice have been described [17]. These studies were approved by the Institutional Animal Care and Use Committee. B cells were isolated from total splenocytes by negative selection using the EasySep® mouse B-cell enrichment kit (StemCell Technologies, Vancouver, Canada). Greater than 90% purity was achieved based on CD19 staining (data not shown). The following cell lines were used: BμMyc.GKO.1, a B-cell lymphoma cell line with an immature B-cell phenotype derived from GILT$^{-/-}$ Eμ-myc transgenic mice [16], and human embryonic kidney 293T cells (American Type Culture Collection, Manassas, VA, USA).

Confocal microscopy

Primary B cells were plated onto alcian blue-coated cover slips and fixed with 3.7% formaldehyde. For LAMP-1 staining, cells were permeabilized with 0.05% saponin. For CatS staining, cells were permeabilized with methanol and 0.05% Triton-X. Cells were stained with rabbit anti-mouse GILT serum followed by either Alexa Fluor 555 goat anti-rabbit IgG (H+L) or Alexa Fluor 488 goat anti-rabbit IgG (H+L). CatS was detected with goat anti-mouse CatS polyclonal Ab (M-19, SantaCruz Biotechnology, Inc., Santa Cruz, CA, USA) followed by Alexa Fluor 555 donkey anti-goat IgG (H+L) (Invitrogen, Carlsbad, CA, USA), and LAMP-1 was probed using Alexa Fluor 488 anti-mouse LAMP-1 mAb (clone 1D4B, BioLegend, San Diego, CA, USA). Nuclei were detected with Hoechst 33342 (Invitrogen). Images were collected using a Zeiss LSM 710 confocal microscope and analyzed with Zen LE software (Carl Zeiss Microimaging Inc., Thornwood, NY). Images of single sections and Z-stacks of 12–24 optical sections with 0.3–0.8 μm increments were taken of each slide. Quantification of the extent of colocalization was determined using the National Institutes of Health ImageJ software (freeware available from http://rsbweb.nih.gov/ij/) with JACoP plugin default settings [46]. Specifically, images of over 200 single cells were used to determine the overlap of signals, as reported by the Manders coefficient [47].

Immunoblotting

Cells were lysed with 1% Triton X-100 in TBS for 30 min on ice. Thymuses were disrupted by sonication and lysed in 2% Triton X-100 in 2× TBS for 15 min on ice. Indicated amounts of postnuclear supernatants were resolved by SDS-PAGE (PAGEr® Gold Tris-Glycine 4–20% polyacrylamide gel, Lonza Rockland Inc., Rockland, ME, USA) and electrophoretically transferred to Immobilon-P membrane (Millipore, Bedford, MA, USA). The membrane was blocked in PBS with 0.1–0.2% Tween-20 and 5% dehydrated milk and then incubated with primary Ab. CatS, H2-Mα, H2-Oβ, and CatL were detected under reducing conditions with goat anti-CatS polyclonal Ab (0.4 μg/mL), mouse anti-HLA-DMα mAb (1 μg/mL, YoDMA.1, generously provided by Dr. L. K. Denzin [22]), rabbit anti-H2-

Oβ polyclonal Ab (1 μg/mL, R.Ob/c, generously provided by Dr. L. K. Denzin [48]), and rabbit anti-CatL serum (1:21 000, kind gift from Dr. A. H. Erickson [35]), respectively. GILT was detected under nonreducing conditions with rabbit anti-human GILT serum (1:2000, kindly provided by Dr. P. Cresswell [23]). Rat anti-GRP94 mAb (0.2 μg/mL, Enzo Life Sciences, Plymouth Meeting, PA, USA) was used as a loading control. Membranes were incubated with HRP-conjugated goat anti-rat, bovine anti-goat, goat anti-rabbit, or goat anti-mouse IgG (1:2500–1:10 000, Jackson ImmunoResearch Laboratories, West Grove, PA) followed by enhanced chemiluminescent substrate (SuperSignal West Pico; Pierce, Rockford, IL, USA or Western Bright ECL; Advansta, Menlo Park, CA) and exposure to film. For cycloheximide treatment, cells were treated with 10 μg/mL cycloheximide (Sigma, St. Louis, MO, USA) for the indicated time periods. Band intensities were determined using Quantity One software (Bio-Rad, Hercules, CA, USA), and relative protein expression was calculated by (intensity of protein of interest–background)/(GRP94 intensity-background). For quantification over time following cycloheximide treatment, protein expression is graphed relative to expression at time zero (set to 1).

Quantitative real-time PCR analysis

RNA was isolated from single-cell suspensions using QiaShredder and the RNeasy Mini kit (Qiagen, Valencia, CA, USA). Total RNA (2 μg) was reverse-transcribed into cDNA using the iScript cDNA Synthesis kit (Bio-Rad). Reactions were performed using Power SYBR® Green PCR master mix (Applied Biosystems, Carlsbad, CA, USA), 150 nM of each primer, and 25 ng cDNA. Amplification was carried out in an Applied Biosystem 7500 Fast Real-Time PCR System for 35 cycles of 95°C denaturation for 15 s, 59°C annealing for 1 min, and 72°C for 1 min. CatS transcript levels were assessed using the exon 6–7 amplifying primers 5′-GCC ATT CCT CCT TCT TCT TC-3′ and 5′-CCA TAG CCA ACC ACA AGA AC-3′, and GAPDH was detected using exon 2–3 primers 5′-AAT GGT GAA GGT CGG TGT GAA C-3′, and 5′-ACA ATC TCC ACT TTG CCA CTG C-3′. The ΔΔCt method was used to calculate fold change in CatS mRNA expression in GILT$^{-/-}$ relative to WT mice normalizing to GAPDH.

Retroviral transduction

The murine stem cell virus-based MigR2 retroviral vectors encoding WT and mutant GILT were previously generated [16]. Supporting Information Fig. 3 shows a map of this vector. Retroviral transduction of GILT-deficient BμMyc.GKO.1 B cells was performed as described [16]. The 293T cells were cotransfected with the MigR2 retroviral vector and pCLeco encoding gag, pol and env cDNAs using Lipofectamine 2000 (Invitrogen). Culture supernatants containing retrovirus were collected after 48 and 72 h at 32°C, diluted 1:2 with medium supplemented with polybrene (8 μg/mL final), and added to BμMyc.GKO.1 cells followed by centrifugation for 90 min at 1258 × *g* at 32°C. Transduced cells were cultured overnight at 32°C and then maintained at 37°C. Transduction efficiency was determined by flow cytometric analysis for human tailless CD2, a reporter expressed under an internal ribosome entry site element (Supporting Information Fig. 2). In each experiment comparing the effect of WT and mutant GILT expression on CatS levels, the transduction efficiency with vectors encoding WT and mutant GILT was greater than 90%. If the transduction efficiency was less than 90%, the transduction was repeated, or the cells were FACS sorted for high CD2 expression. Equivalent GILT expression was confirmed by Western blot, as in Fig. 3A.

Protease activity assay

CatS, CatB, and CatL protease activity was measured with a fluorescence-based assay using selective substrate sequences labeled with AFC, according to the manufacturer's protocol (Bio-Vision Mountain View, CA, USA). CatS, CatB, and CatL selective substrates used

were Ac-valine-valine-arginine (VVR)-AFC, Ac-arginine-arginine (RR)-AFC, and Ac-phenylalanine-arginine (FR)-AFC, respectively. Cleavage of the synthetic substrate releases free AFC. Cat inhibitor *Z*-phenylalanine-phenylalanine (FF)-fluoromethyl ketone (FMK) (20 μM final) was added to selected wells. Samples were incubated at 37°C in a fluorimeter, and relative fluorescence units were measured at 15-min intervals. Fluorescence of free AFC was detected at λexc 400 nm and λemi 505 nm. Cat activity was expressed as μM free AFC as determined by generating a standard curve using free AFC under assay conditions.

Supplementary Material

Refer to Web version on PubMed Central for supplementary material.

Acknowledgments

This work was supported in part by National Institutes of Health grants K08-AR054388 (to KTH) and T32-CA09213 (to HPY) and a grant from the Arizona Biomedical Research Commission (to KTH). We thank Dr. Lonnie Lybarger, Dr. Kathleen Corcoran, and Dr. Maurice Jabbour for technical assistance, and Dr. Lybarger for critical review of the manuscript.

Abbreviations

AFC	amino-4-trifluoromethyl coumarin
Cat	cathepsin
CLIP	class II-associated invariant chain peptides
GILT	gamma-interferon-inducible lysosomal thiol reductase
LAMP-1	lysosome-associated membrane protein-1

References

1. Rocha N, Neefjes J. MHC class II molecules on the move for successful antigen presentation. EMBO J. 2008; 27:1–5. [PubMed: 18046453]
2. Anderson MS, Miller J. Invariant chain can function as a chaperone protein for class II major histocompatibility complex molecules. Proc Natl Acad Sci USA. 1992; 89:2282–2286. [PubMed: 1549594]
3. Bakke O, Dobberstein B. MHC class II-associated invariant chain contains a sorting signal for endosomal compartments. Cell. 1990; 63:707–716. [PubMed: 2121367]
4. Ghosh P, Amaya M, Mellins E, Wiley DC. The structure of an intermediate in class II MHC maturation: CLIP bound to HLA-DR3. Nature. 1995; 378:457–462. [PubMed: 7477400]
5. Lotteau V, Teyton L, Peleraux A, Nilsson T, Karlsson L, Schmid SL, Quaranta V, et al. Intracellular transport of class II MHC molecules directed by invariant chain. Nature. 1990; 348:600–605. [PubMed: 2250716]
6. Morkowski S, Goldrath AW, Eastman S, Ramachandra L, Freed DC, Whiteley P, Rudensky A. T cell recognition of major histocompatibility complex class II complexes with invariant chain processing intermediates. J Exp Med. 1995; 182:1403–1413. [PubMed: 7595211]
7. Romagnoli P, Germain RN. The CLIP region of invariant chain plays a critical role in regulating major histocompatibility complex class II folding, transport, and peptide occupancy. J Exp Med. 1994; 180:1107–1113. [PubMed: 8064228]
8. Tulp A, Verwoerd D, Dobberstein B, Ploegh HL, Pieters J. Isolation and characterization of the intracellular MHC class II compartment. Nature. 1994; 369:120–126. [PubMed: 8177317]
9. West MA, Lucocq JM, Watts C. Antigen processing and class II MHC peptide-loading compartments in human B-lymphoblastoid cells. Nature. 1994; 369:147–151. [PubMed: 8177319]

10. Maric MA, Taylor MD, Blum JS. Endosomal aspartic proteinases are required for invariant-chain processing. Proc Natl Acad Sci USA. 1994; 91:2171–2175. [PubMed: 8134367]
11. Neefjes JJ, Ploegh HL. Inhibition of endosomal proteolytic activity by leupeptin blocks surface expression of MHC class II molecules and their conversion to SDS resistance alpha beta heterodimers in endosomes. EMBO J. 1992; 11:411–416. [PubMed: 1311249]
12. Riese RJ, Wolf PR, Bromme D, Natkin LR, Villadangos JA, Ploegh HL, Chapman HA. Essential role for cathepsin S in MHC class II-associated invariant chain processing and peptide loading. Immunity. 1996; 4:357–366. [PubMed: 8612130]
13. Nakagawa TY, Brissette WH, Lira PD, Griffiths RJ, Petrushova N, Stock J, McNeish JD, et al. Impaired invariant chain degradation and antigen presentation and diminished collagen-induced arthritis in cathepsin S null mice. Immunity. 1999; 10:207–217. [PubMed: 10072073]
14. Shi GP, Villadangos JA, Dranoff G, Small C, Gu L, Haley KJ, Riese R, et al. Cathepsin S required for normal MHC class II peptide loading and germinal center development. Immunity. 1999; 10:197–206. [PubMed: 10072072]
15. Riese RJ, Mitchell RN, Villadangos JA, Shi GP, Palmer JT, Karp ER, De Sanctis GT, et al. Cathepsin S activity regulates antigen presentation and immunity. J Clin Invest. 1998; 101:2351–2363. [PubMed: 9616206]
16. Hastings KT, Lackman RL, Cresswell P. Functional requirements for the lysosomal thiol reductase GILT in MHC class II-restricted antigen processing. J Immunol. 2006; 177:8569–8577. [PubMed: 17142755]
17. Maric M, Arunachalam B, Phan UT, Dong C, Garrett WS, Cannon KS, Alfonso C, et al. Defective antigen processing in GILT-free mice. Science. 2001; 294:1361–1365. [PubMed: 11701933]
18. Rausch MP, Irvine KR, Antony PA, Restifo NP, Cresswell P, Hastings KT. GILT accelerates autoimmunity to the melanoma antigen tyrosinase-related protein 1. J Immunol. 2010; 185:2828–2835. [PubMed: 20668223]
19. Denzin LK, Cresswell P. HLA-DM induces CLIP dissociation from MHC class II alpha beta dimers and facilitates peptide loading. Cell. 1995; 82:155–165. [PubMed: 7606781]
20. Denzin LK, Hammond C, Cresswell P. HLA-DM interactions with intermediates in HLA-DR maturation and a role for HLA-DM in stabilizing empty HLA-DR molecules. J Exp Med. 1996; 184:2153–2165. [PubMed: 8976171]
21. Denzin LK, Sant'Angelo DB, Hammond C, Surman MJ, Cresswell P. Negative regulation by HLA-DO of MHC class II-restricted antigen processing. Science. 1997; 278:106–109. [PubMed: 9311912]
22. Fallas JL, Tobin HM, Lou O, Guo D, Sant'Angelo DB, Denzin LK. Ectopic expression of HLA-DO in mouse dendritic cells diminishes MHC class II antigen presentation. J Immunol. 2004; 173:1549–1560. [PubMed: 15265882]
23. Arunachalam B, Phan UT, Geuze HJ, Cresswell P. Enzymatic reduction of disulfide bonds in lysosomes: characterization of a gamma-interferon-inducible lysosomal thiol reductase (GILT). Proc Natl Acad Sci USA. 2000; 97:745–750. [PubMed: 10639150]
24. Haque MA, Li P, Jackson SK, Zarour HM, Hawes JW, Phan UT, Maric M, et al. Absence of γ-interferon-inducible lysosomal thiol reductase in melanomas disrupts T cell recognition of select immunodominant epitopes. J Exp Med. 2002; 195:1267–1277. [PubMed: 12021307]
25. Honey K, Duff M, Beers C, Brissette WH, Elliott EA, Peters C, Maric M, et al. Cathepsin S regulates the expression of cathepsin L and the turnover of γ-interferon-inducible lysosomal thiol reductase in B lymphocytes. J Biol Chem. 2001; 276:22573–22578. [PubMed: 11306582]
26. Phan UT, Arunachalam B, Cresswell P. Gamma-interferon-inducible lysosomal thiol reductase (GILT). Maturation, activity, and mechanism of action. J Biol Chem. 2000; 275:25907–25914. [PubMed: 10852914]
27. Arunachalam B, Pan M, Cresswell P. Intracellular formation and cell surface expression of a complex of an intact lysosomal protein and MHC class II molecules. J Immunol. 1998; 160:5797–5806. [PubMed: 9637490]
28. Singh R, Cresswell P. Defective cross-presentation of viral antigens in GILT-free mice. Science. 2010; 328:1394–1398. [PubMed: 20538950]

29. Rausch MP, Hastings KT. GILT modulates CD4(+) T-cell tolerance to the melanocyte differentiation antigen tyrosinase-related protein 1. J Invest Dermatol. 2012; 132:154–162. [PubMed: 21833020]
30. Goldstein OG, Hajiaghamohseni LM, Amria S, Sundaram K, Reddy SV, Haque A. Gamma-IFN-inducible-lysosomal thiol reductase modulates acidic proteases and HLA class II antigen processing in melanoma. Cancer Immunol Immunother. 2008; 57:1461–1470. [PubMed: 18343923]
31. Deussing J, Roth W, Saftig P, Peters C, Ploegh HL, Villadangos JA. Cathepsins B and D are dispensable for major histocompatibility complex class II-mediated antigen presentation. Proc Natl Acad Sci USA. 1998; 95:4516–4521. [PubMed: 9539769]
32. Villadangos JA, Riese RJ, Peters C, Chapman HA, Ploegh HL. Degradation of mouse invariant chain: roles of cathepsins S and D and the influence of major histocompatibility complex polymorphism. J Exp Med. 1997; 186:549–560. [PubMed: 9254653]
33. Blander JM, Medzhitov R. Toll-dependent selection of microbial antigens for presentation by dendritic cells. Nature. 2006; 440:808–812. [PubMed: 16489357]
34. Nakagawa T, Roth W, Wong P, Nelson A, Farr A, Deussing J, Villadangos JA, et al. Cathepsin L: critical role in Ii degradation and CD4 T cell selection in the thymus. Science. 1998; 280:450–453. [PubMed: 9545226]
35. Portnoy DA, Erickson AH, Kochan J, Ravetch JV, Unkeless JC. Cloning and characterization of a mouse cysteine proteinase. J Biol Chem. 1986; 261:14697–14703. [PubMed: 3533924]
36. Turkenburg JP, Lamers MB, Brzozowski AM, Wright LM, Hubbard RE, Sturt SL, Williams DH. Structure of a Cys25–>Ser mutant of human cathepsin S. Acta Crystallogr D Biol Crystallogr. 2002; 58:451–455. [PubMed: 11856830]
37. Lennon-Dumenil AM, Bakker AH, Maehr R, Fiebiger E, Overkleeft HS, Rosemblatt M, Ploegh HL, et al. Analysis of protease activity in live antigen-presenting cells shows regulation of the phagosomal proteolytic contents during dendritic cell activation. J Exp Med. 2002; 196:529–540. [PubMed: 12186844]
38. Sealy R, Chaka W, Surman S, Brown SA, Cresswell P, Hurwitz JL. Target peptide sequence within infectious human immunodeficiency virus type 1 does not ensure envelope-specific T-helper cell reactivation: influences of cysteine protease and gamma interferon-induced thiol reductase activities. Clin Vaccine Immunol. 2008; 15:713–719. [PubMed: 18235043]
39. Vidard L, Rock KL, Benacerraf B. The generation of immunogenic peptides can be selectively increased or decreased by proteolytic enzyme inhibitors. J Immunol. 1991; 147:1786–1791. [PubMed: 1890304]
40. Trombetta ES, Ebersold M, Garrett W, Pypaert M, Mellman I. Activation of lysosomal function during dendritic cell maturation. Science. 2003; 299:1400–1403. [PubMed: 12610307]
41. Bogunovic B, Srinivasan P, Ueda Y, Tomita Y, Maric M. Comparative quantitative mass spectrometry analysis of MHC class II-associated peptides reveals a role of GILT in formation of self-peptide repertoire. PLoS One. 2010; 5:e10599. [PubMed: 20485683]
42. Saegusa K, Ishimaru N, Yanagi K, Arakaki R, Ogawa K, Saito I, Katunuma N, et al. Cathepsin S inhibitor prevents autoantigen presentation and autoimmunity. J Clin Invest. 2002; 110:361–369. [PubMed: 12163455]
43. Baugh M, Black D, Westwood P, Kinghorn E, McGregor K, Bruin J, Hamilton W, et al. Therapeutic dosing of an orally active, selective cathepsin S inhibitor suppresses disease in models of autoimmunity. J Autoimmun. 2011; 36:201–209. [PubMed: 21439785]
44. Pierre P, Mellman I. Developmental regulation of invariant chain proteolysis controls MHC class II trafficking in mouse dendritic cells. Cell. 1998; 93:1135–1145. [PubMed: 9657147]
45. El-Sukkari D, Wilson NS, Hakansson K, Steptoe RJ, Grubb A, Shortman K, Villadangos JA. The protease inhibitor cystatin C is differentially expressed among dendritic cell populations, but does not control antigen presentation. J Immunol. 2003; 171:5003–5011. [PubMed: 14607896]
46. Bolte S, Cordelieres FP. A guided tour into subcellular colocalization analysis in light microscopy. J Microsc. 2006; 224:213–232. [PubMed: 17210054]

47. Manders EM, Stap J, Brakenhoff GJ, van Driel R, Aten JA. Dynamics of three-dimensional replication patterns during the S-phase, analysed by double labelling of DNA and confocal microscopy. J Cell Sci. 1992; 103(Pt 3):857–862. [PubMed: 1478975]

48. Fallas JL, Yi W, Draghi NA, O'Rourke HM, Denzin LK. Expression patterns of H2-O in mouse B cells and dendritic cells correlate with cell function. J Immunol. 2007; 178:1488–1497. [PubMed: 17237397]

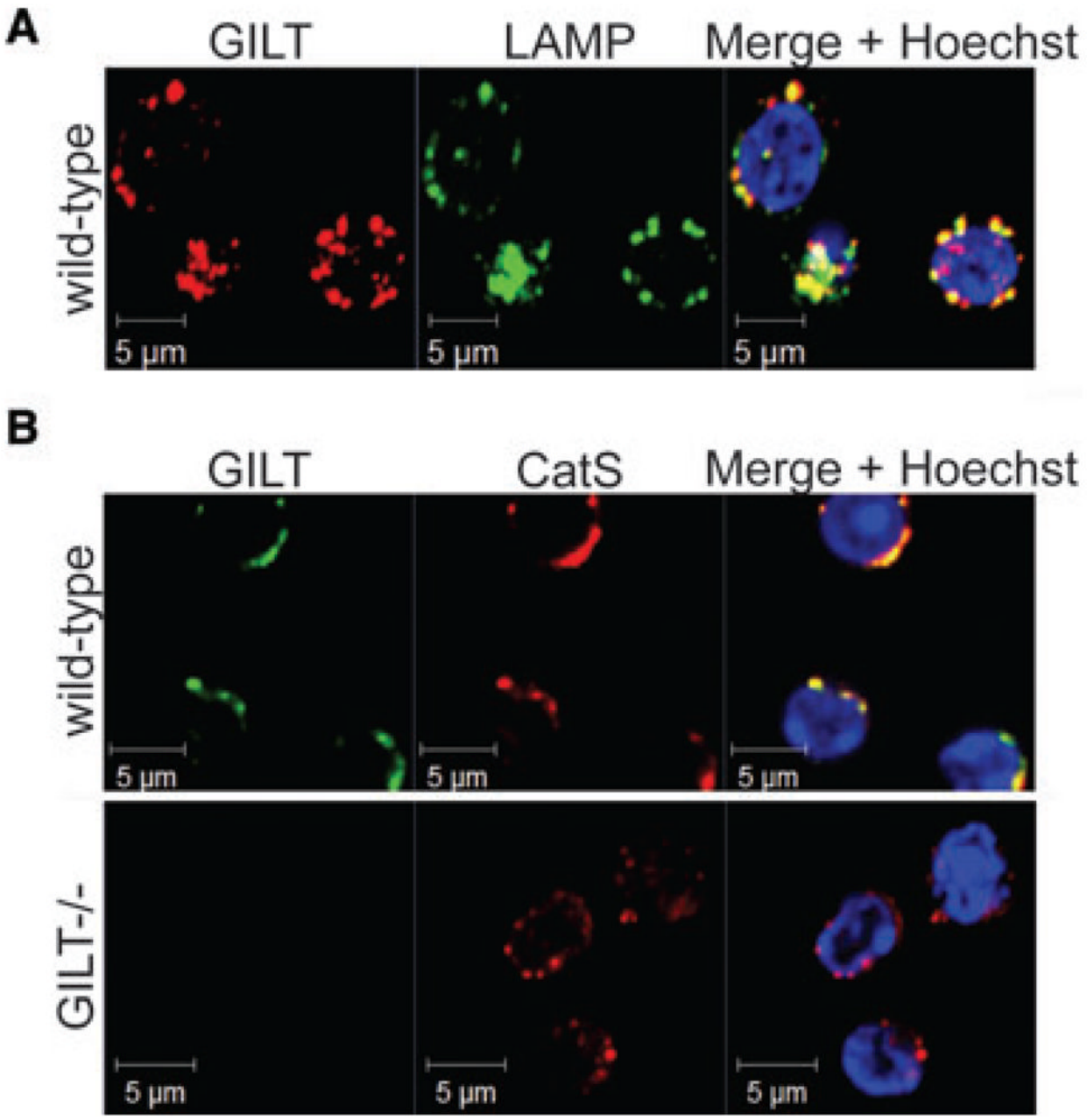

Figure 1.

GILT and CatS colocalize in lysosomes of primary B cells. Confocal microscopy of WT and GILT$^{-/-}$ primary B cells isolated by magnetic bead negative selection from murine splenocytes. Cells were fixed, permeabilized, and stained with (A) rabbit anti-GILT serum followed by Alexa Fluor 555-conjugated goat anti-rabbit (red, left), Alexa Fluor 488-conjugated anti-LAMP-1 (green, middle) and Hoechst (blue, right), or (B) rabbit anti-GILT serum followed by Alexa Fluor 488-conjugated goat anti-rabbit (green, left), goat anti-CatS followed by Alexa Fluor 555-conjugated donkey anti-goat (red, middle) and Hoechst (blue, right). Merged images (yellow) along with Hoechst are shown (right). Photographs were taken with 63× magnification under oil, and scale bar indicates 5 μm. Images are from a single 0.6 μm section. Data are representative of at least three independent experiments.

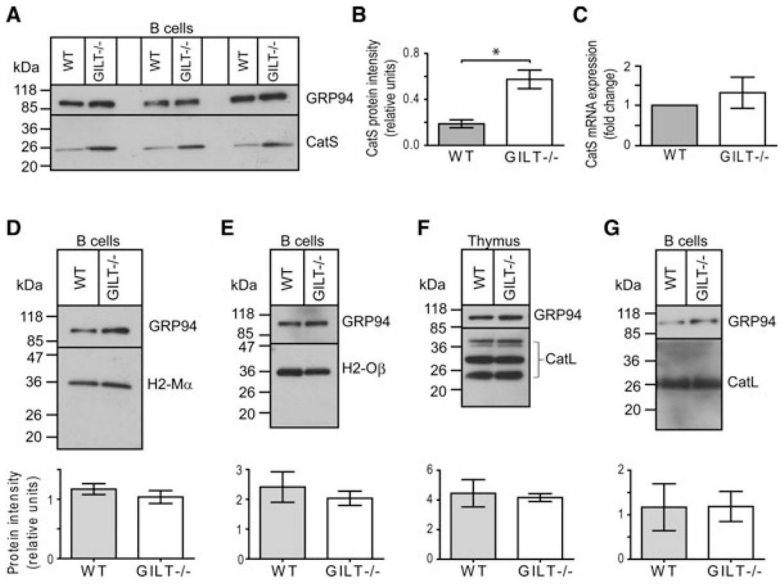

Figure 2.

GILT acts posttranscriptionally to decrease the steady-state protein expression of CatS in primary B cells. Immunoblot analysis of (A) CatS, (D) H2-M, (E) H2-O, and (F and G) CatL in detergent lysates of WT and GILT$^{-/-}$ primary B cells (A, D, E, and G) or thymus (F). Postnuclear supernatants of lysates (9, 15, 5, 22, and 15 μg/lane for A, D, E, F, and G, respectively) were resolved by 4–20% gradient SDS-PAGE under reducing conditions and probed with goat anti-CatS polyclonal Ab, mouse anti-H2-Mα mAb, rabbit anti-H2-Oβ Ab, or rabbit anti-CatL serum. GRP94 served as a loading control. (A) Immunoblot analysis and (B) densitometry of CatS expression are shown. (B) Band intensities were estimated using Quantity One software, and CatS expression was normalized to GRP94 expression. Data are shown as the mean ± SEM of three sets of lysates from three performed experiments. $^{*}p < 0.05$, independent sample Student's *t*-test. (C) Quantitative RT-PCR of CatS in primary B cells showed similar CatS mRNA transcript levels in WT and GILT$^{-/-}$ B cells. CatS mRNA expression was normalized to GAPDH mRNA expression and expressed as fold change relative to expression in WT cells. Data are shown as the mean ± SD of three independent sets of WT and GILT$^{-/-}$ B cells. (D–G) Immunoblot analysis and densitometry of H2-M, H2–O, and CatL are shown. Data are shown as the mean ± SEM of the signal intensities in WT and GILT$^{-/-}$ B-cell lysates pooled from four independent experiments in (D), three independent experiments in (E and F) and six independent experiments in (G).

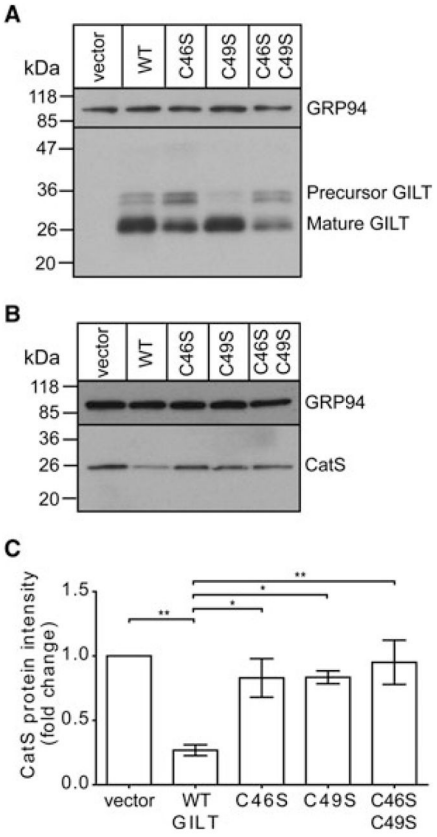

Figure 3.

GILT's reductase active site is necessary for diminished CatS steady-state protein levels. Immunoblot analysis of (A) GILT and (B) CatS protein expression in BμMyc.GKO.1 cells stably transduced with vector alone, WT GILT, or mutant C46S, C49S, or C46SC49S GILT. Post-nuclear supernatants of lysates (25 μg/lane) were resolved by 4–20% gradient SDS-PAGE under nonreducing (GILT) or reducing (CatS) conditions and probed with rabbit anti-GILT serum or goat anti-CatS Ab. GRP94 served as a loading control. (C) CatS expression was normalized to GRP94 and shown relative to cells transduced with vector alone. Data are shown as the mean ± SEM of the signal intensities from lysates of BμMyc.GKO.1 cells transduced with vector alone, WT, or mutant GILT from five independent experiments. $^{*}p < 0.05$, $^{**}p < 0.01$, ANOVA with a Bonferroni adjustment for multiple comparisons.

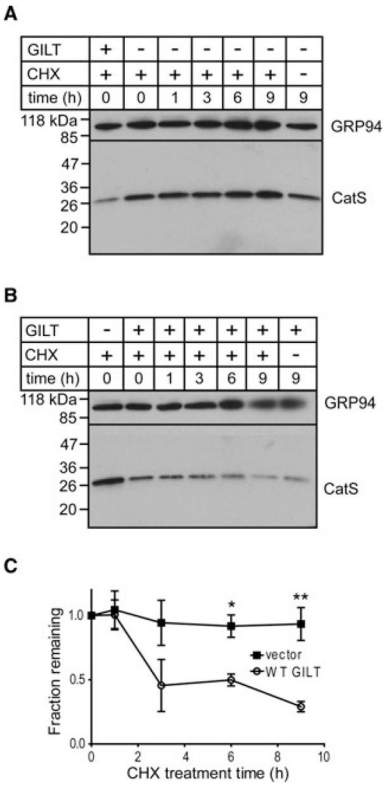

Figure 4.

GILT decreases the half-life of CatS. (A and B) Immunoblot analysis of CatS protein expression in GILT-deficient BμMyc.GKO.1 cells stably transduced with vector alone (GILT -) or WT GILT (GILT +). Cells were treated with cycloheximide (CHX +) or DMSO (CHX -) for the indicated times. Postnuclear supernatants of lysates (40 μg/lane) were resolved by 4–20% gradient SDS-PAGE under reducing conditions and probed with goat anti-CatS Ab and rat anti-GPR94Ab, as a loading control. (C) CatS expression was quantified, normalized to GRP94, and shown relative to expression at 0 h. Data are shown as the mean ± SEM of vector alone or WT GILT samples pooled from three independent experiments. $^{*}p < 0.05$, $^{**}p < 0.01$, Student's *t*-test.

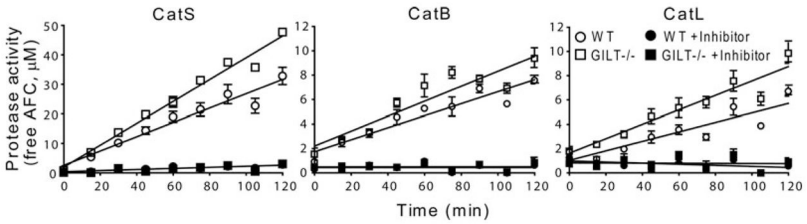

Figure 5.

GILT decreases the proteolysis of a CatS-selective substrate. CatS, CatB, and CatL activity was measured in lysates (1×10^6 cell equivalents) from primary B cells isolated from WT and GILT$^{-/-}$ murine splenocytes based upon the cleavage of a CatS, CatB, or CatL-selective substrate. Cathepsin inhibitor was included as indicated. Activity is expressed as the concentration of the released fluorophore (free AFC, μM). Data are shown as the mean ± SEM of triplicates from one experiment representative of two independent experiments. Lines represent the result of linear regression. The scale for CatB and CatL activity is smaller to highlight any differences between the activity of WT and GILT$^{-/-}$ lysates. Comparison of the slopes by ANCOVA revealed a significant difference in CatS ($p < 0.0001$) and CatL ($p < 0.01$) activity between WT and GILT$^{-/-}$ B-cell lysates.